Ultrafast dynamics of adenine following XUV ionization

Erik P. Månsson[1,2], Simone Latini[3], Fabio Covito[3], Vincent Wanie[1,2,4], Mara Galli[1,5], Enrico Perfetto[6,7], Gianluca Stefanucci[7,8], Umberto De Giovannini[3,9], Mattea C. Castrovilli[2,10], Andrea Trabattoni[1], Fabio Frassetto[11], Luca Poletto[11], Jason B. Greenwood[12], François Légaré[4], Mauro Nisoli[2,5], Angel Rubio[3,13] and Francesca Calegari[1,2,14]

[1] Center for Free-Electron Laser Science CFEL, Deutsches Elektronen-Synchrotron DESY, Notkestrasse 85, 22607 Hamburg, Germany. [2] Inst. for Photonics and Nanotechnologies CNR-IFN, P.za L. da Vinci 32, 20133 Milano, Italy. [3] Max Planck Institute for the Structure and Dynamics of Matter and Center for Free Electron Laser Science, 22761 Hamburg, Germany. [4] INRS-EMT, 1650 Blvd. Lionel Boulet J3X 1S2, Varennes, Canada. [5] Department of Physics, Politecnico di Milano, Piazza L. da Vinci 32, 20133 Milano, Italy. [6] CNR-ISM, Division of Ultrafast Processes in Materials (FLASHit), Area della ricerca di Roma 1, Via Salaria Km 29.3, I-00016 Monterotondo Scalo, Italy. [7] Dipartimento di Fisica, Università di Roma Tor Vergata, Via della Ricerca Scientifica, 00133 Roma, Italy. [8] INFN, Sezione di Roma Tor Vergata, Via della Ricerca Scientifica 1, 00133 Roma, Italy. [9] Dipartimento di Fisica e Chimica, Università degli Studi di Palermo, Via Archirafi 36, I-90123, Palermo, Italy. [10] Istituto di Struttura della Materia-CNR, (ISM-CNR), Area della Ricerca di Roma 1, 00015, Monterotondo, Italy. [11] Inst. for Photonics and Nanotechnologies CNR-IFN, Via Trasea 7, 35131 Padova, Italy. [12] Centre for Plasma Physics, School of Maths and Physics, Queen's University Belfast, BT7 1NN, Belfast, UK. [13] Center for Computational Quantum Physics (CCQ), The Flatiron Institute, 162 Fifth avenue, New York NY 10010, USA. [14] Institut für Experimentalphysik, Universität Hamburg, Luruper Chaussee 149, D-22761 Hamburg, Germany.

E-mail: `francesca.calegari@desy.de`

February 9, 2022

Abstract. The dynamics of biologically relevant molecules exposed to ionizing radiation contains many facets and spans several orders of magnitude in time and energy. In the extreme ultraviolet (XUV) spectral range, multi-electronic phenomena and bands of correlated states with inner-valence holes must be accounted for in addition to a plethora of vibrational modes and available dissociation channels. To be able to track changes in charge density and bond length during ultrafast reactions is an important endeavour towards more general abilities to simulate and control photochemical processes, possibly inspired by those that have evolved biologically. Using attosecond XUV and few-femtosecond near-infrared pulses, we report on electronic and vibrational dynamics in the adenine nucleobase cation. The time-dependent yields of parent and fragment ions in mass spectra are analysed to extract exponential time constants and oscillation periods. Together with time-dependent density functional theory and ab-initio Green's function methods this allows different vibrational and electronic processes to be identified and quantified. Beyond providing further insights into the XUV-induced dynamics of an important nucleobase, our work demonstrates that yields of specific dissociation outcomes can be influenced by sufficiently well-timed ultrashort pulses, and provides insight to multi-electronic and dissociative dynamics of a nucleobase in an energy range little explored to date with high temporal resolution.

Submitted to: *J. Phys. Photonics*

1. Introduction

The localization and transport of charge is essential for many photoreactions in biomolecules and functional materials. Just as femtosecond laser technology led to the femtochemistry paradigm, where coherent vibrational wavepackets can be excited and the nuclear motion of molecules be tracked in real time[1, 2], attosecond technology is making it possible to time-resolve electronic dynamics, including multi-electronic transitions with core- or inner-valence holes[3, 4, 5, 6] and charge migration across a molecule[7, 8, 9]. There is a great interest in utilizing such pulses of light to understand if and how the speed and efficiency of reactions can be improved by better utilizing charge migration and other electronic dynamics, a research field that can be called "attochemistry"[10, 11, 12, 13].

Attosecond pulses are generated via the high-harmonic generation process[14, 15], where a near-infrared (NIR) laser pulse is focused to tunnel-ionize a medium and accelerate electrons away from and then back to their parent ion. The excess kinetic energy of each recombining electron becomes emitted as a photon, which may extend into the extreme ultraviolet (XUV) or soft x-ray regime, depending on the driving laser and medium. Crucially, coherence is preserved from the driving NIR laser to and within the generated attosecond pulse spectrum, allowing pump–probe experiments with sub-femtosecond precision. Attosecond methods based on photoelectron spectroscopy can measure pulse durations[16, 17, 18] or time-delays in XUV photoionization processes[19, 20, 21, 22, 23, 24, 25, 26] and in the subsequent NIR-probing[27]. Spectroscopy on the initial photoelectron is however not sensitive to later dynamics *within* the molecule, for which transient absorption spectroscopy[28, 29] and pump–probe mass spectrometry are often used[30, 31, 32, 33].

Charge migration is defined as a net change in electron or hole probability density within a molecule without any accompanying motion of nuclei (which would be called charge transfer instead)[34, 35]. In the mid-1990s it was suggested that this occurred in oligopeptides (short chains of amino acids) after site-selective photoionization[36], based on observations of which charged fragment was obtained. Theoretical work for di- and tetrapeptides showed that a hole could transferred already in 1 to 5 fs[37, 38]. Such a redistribution of charge within a molecule can in some cases be achieved through a quantum beat of coherently excited orbitals of different energy, while it in other cases must be described as an intrinsic correlation-driven electronic relaxation that lets the occupation of electronic states evolve over time. Experimentally, the use of an isolated attosecond pulse and few-femtosecond near-infrared (NIR) probing pulse has allowed approximately 4-fs-periodic charge migration to be confirmed within the single amino acids phenylalanine[7] and tryptophan[39, 40, 41].

A related class of biomolecules are DNA-building blocks, such as nucleosides and nucleobases. Attosecond charge migration from one nucleobase to its complementary nucleobase was recently examined in simulations after removing an oxygen-1s electron[42]. Such processes could have direct consequences for the probability of DNA-damage, for which improved control or biological targeting could have applications in radiation therapy of tumours. In general, ionizing radiation is more likely to damage DNA indirectly via radicals and low-energy secondary electrons created when the primary radiation interacts with the much more abundant water molecules in tissue[43, 44, 45]. Although the relaxation of DNA-building blocks after 5-eV ultraviolet photoexcitation has been studied extensively with sub-picosecond resolution[46, 47, 48], time-resolved information about the initial electronic dynamics and its implications for structural integrity is still missing in the 10 to 50 eV energy range relevant for DNA strand-breakage[43, 49]. We have previously reported on the dissociation dynamics of the nucleobase thymine and its nucleoside thymidine ionized by XUV attosecond pulses[50].

In this work, we describe time-resolved electronic and vibrational dynamics of the nucleobase adenine, ionized by 17–35 eV photons. In the first part, we discuss how XUV-induced charge migration in the adenine cation enables the production of *intact* dications. We use additional experimental data beyond our recent report on this phenomenon[6], which to our knowledge constituted the first photoionization study of adenine above the 23.5 eV dication appearance energy[51]. In the second part, we instead examine the *fragment* ions and discuss signatures of different types of vibrational dynamics. Together, the two parts provide complementary information about the femtosecond dynamics in photoionized adenine.

2. Experimental set-up

Carrier–phase stabilized 25 fs pulses from a titanium:sapphire laser are sent through a hollow-core fibre with a pressure gradient of helium for self-phase modulation, and compressed to 4 fs with a central wavelength of about 700 nm (1.77 eV) by chirped mirrors[52, 53]. A beam splitter gives two replicas of this near-infrared (NIR) pulse, one of which is sent through waveplates for polarization gating[54, 55, 56] and focused in a pulsed jet of krypton to generate[14, 15] the extreme ultraviolet (XUV) isolated attosecond pulse. An aluminium filter is then used to block the residual NIR while transmitting most of the XUV[57]. The resulting attosecond pulse has a duration below 300 as and a continuous XUV spectrum from 17 to 35 eV, with the highest spectral intensity near 27 eV[6]. The other part of the NIR-beam is used as probe at an estimated intensity of 1–1.4$\times 10^{13}$ W/cm^2, recombined collinearly using an annular mirror after a piezoelectric delay-stage to achieve a Mach–Zehnder-like interferometer. To reduce most of the thermal drift, an active stabilization system for the delay is locked onto the spatial fringes of a helium:neon laser that is co-propagating through most of the interferometer (giving an in-loop residual RMS error of 20 as).

Adenine was sublimated at 190 °C with helium as carrier and buffer gas, entering the electrostatic time-of-flight mass-spectrometer through a 1 mm skimmer. To avoid detecting the comparably high amount of helium, the microchannel plate and phosphor screen detector voltages were gated. Because this gives a detector efficiency that gradually drops off for the lightest ions, we choose to present only ions with a mass/charge ratio of 25 u or greater.

3. Results and discussion

Results concerning three topics will be presented after an overview of adenine's main fragmentation channels in section 3.1. In section 3.2, we summarize our recent discovery of electronic dynamics that redistributes the charge and allows a stable dication to be produced. Thereafter, we examine onset and decay times of several fragmentation channels in section 3.3 and finally the oscillations in two of them in section 3.4.

3.1. Pump–probe mass spectra

An overview of the mass spectra obtained when adenine (135 u, 8.20 eV ionization energy[60]) is photoionized by an XUV attosecond pulse and probed by a NIR pulse is shown in Figure 1. The ionic fragment with the lowest appearance energy is 108 u (11.3 to 12.3 eV[51, 60, 61]), via the loss of neutral 27 u as depicted in Figure 2(a) [62, 60, 59, 58]. Adenine furthermore exhibits sequential ejection of neutral 27 u CHN-groups, indicated with solid arrows in Figure 1. This gives rise to the fragments $C_nH_nN_n^+$ (n=5 is the parent cation) with appearance energies increasing gradually to 14±0.6 eV[51] for $n = 1$ (a charged 27 u CHN $^+$ fragment). CHN should be seen as a sum formula, referring to either of the HCN or HNC isomers which are usually not distinguished. As exemplified in Figure 2(a & b), some hydrogen migration is necessary for 81 u and 27 u, while (d) shows a shortcut to 54 u by ejecting $C_2H_2N_2$ in one step.

Dashed arrows in Figure 1 indicate a sequence where also the neutral –NH_2 group is lost, explained in Figure 2(e). This sequence ends with the 38 u C_2N^+ fragment whose yield varies considerably in the literature, most likely due to its higher appearance energy of 20–23 eV[51]. Simulations of 70 eV electron-impact-ionization[58] failed to reproduce both 38 u and 27 u ions while they were stronger than the 39 u in an experiment using 14 keV projectiles[63]. This seems consistent with the assignments of 27 and 38 u ions as the end products of long dissociation sequences in Figure 2(b & e), where small perturbations along the way might lead to other outcomes instead.

As evident from Figure 1, XUV-photoionization leads to a high level of fragmentation (81 % of the total yield) regardless of when (and if) probed by the NIR-pulse, indicating the moderate photo-stability of adenine in the 17–35 eV energy range[51]. The dashed blue curve with the NIR pulse before the XUV has the same fragment distribution as the XUV gives on its own[6, supplementary information] but when the NIR pulse is sent after the XUV (solid red curve) it deposits further energy to the molecules ionized or highly excited by the XUV and helps to fragment them into smaller pieces. This is seen more clearly in the difference mass spectrum, as strong enhancements of many small ionic fragments and reduced yields of the larger fragments. The net change is positive, indicating that the NIR not only dissociates but also photoionizes.

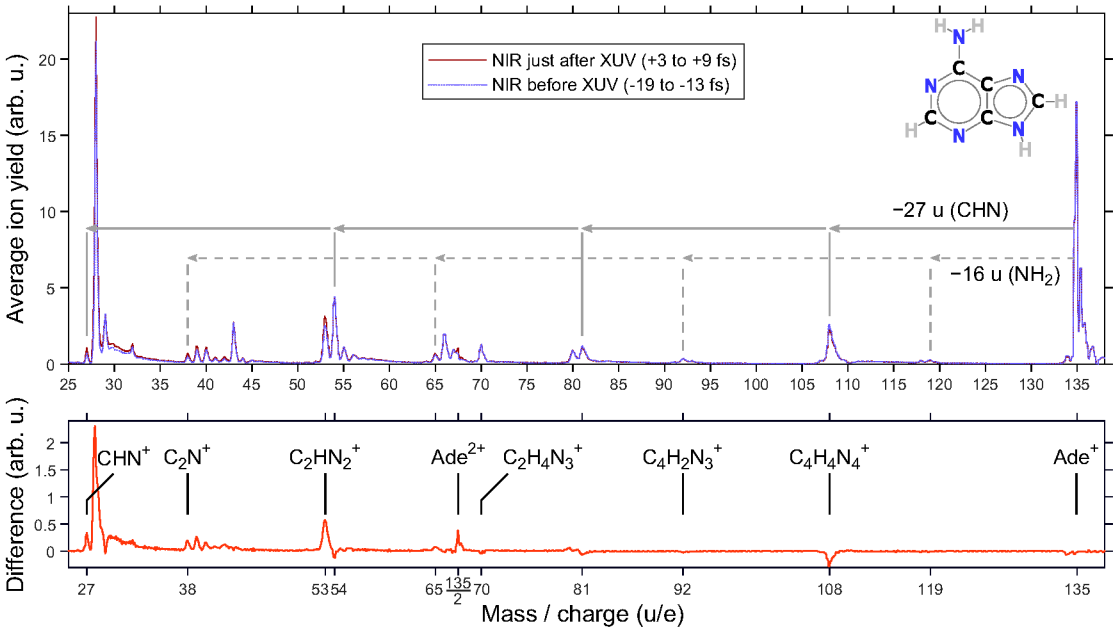

Figure 1. Mass spectra of photoionized adenine. The top panel shows the results of sending the NIR pulse after or before the XUV pulse, and the bottom panel makes the small but meaningful difference between them visible. With the NIR just after the XUV, the adenine dication appears and the yield is increased for small fragments and somewhat reduced for large fragments (the net increase is 6 %). The structure of neutral adenine is shown as an inset. Each mass bin is $\frac{1}{16}$ u wide and the ion yield unit is chosen such that a delay-averaged mass spectrum has a sum of 1000.

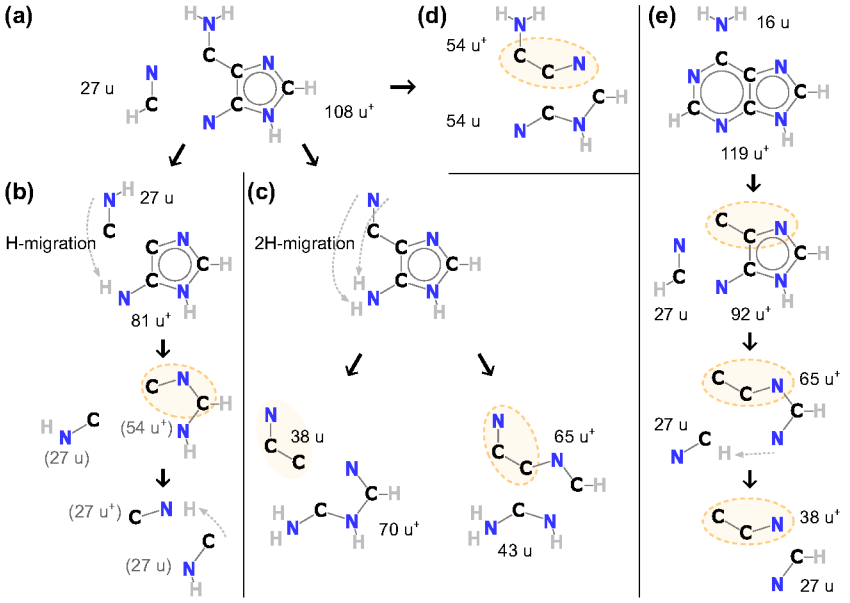

Figure 2. Dissociation paths of interest. (a) The dissociation requiring the least energy is ejection of neutral HCN [58, 59]. (b) The resulting 108 u ion can further dissociate by successive HCN/HNC-losses (solid arrows in Figure 1) and possibly reach a charged HNC^+ (the steps beyond the 81 u ion[59] are illustrated without precise theoretical support). (c) A 2H-migration is likely to occur in the 108 u ion, after which two dissociations are shown: neutral 38 u with a 70 u ion[60] or neutral 43 u and a 65 u ion[59] (from which ionic 38 u would only require a single bond-breakage). (d) By splitting the 108 u in half[58] another 54 u isomer than in (b) can be produced. (e) Dissociations involving loss of the NH2-group (here assumed as first step) and any number of HCN-groups (dashed arrows in Figure 1), leading to the 38 u ion [60]. Throughout the figure, shaded (dashed) ellipses indicate alternative origins of 38 u (ions) that require breaking one or two bonds.

On its own, the NIR-pulse can produce parent cations through multi-photon ionization but essentially without fragmentation (1 % of the total yield was 108 u).

To extract physical information from a pump–probe experiment, we will use a curve model based on a differential equation system where the probed state is being populated via transitions with a total rate of $1/\tau_1$ and simultaneously decaying with a total rate of $1/\tau_2$ to non-observable states. Under the assumption that $0 \leq \tau_1 < \tau_2$, the solution has two exponential terms and can be analytically convoluted with a Gaussian to represent the finite pulse durations[6, Supplementary Information]. In the limiting case of $\tau_1 \approx 0$, the model simplifies to a step function that decays with lifetime τ_2, and represents probing from a state immediately populated by the short XUV-pulse. In the opposite case of probing a slowly populated final-state which does not decay within the scan range ($\tau_2 \to \infty$), the model can instead reduce to $(1 - \mathrm{e}^{-t/\tau_1})h$. The step height h may be either positive or negative. Further details can be found in Appendix A.

3.2. Correlated electron dynamics in the adenine cation

In addition to the enhanced dissociation described in the previous section, we find that a delayed NIR-pulse also leads to the production of adenine^{2+}, the parent dication where no bond is broken but an extra electron is removed. Energetically, this outcome should be allowed already by the 17–35 eV XUV-pulse on its own, since, a dication appearance energy of 23.5 ± 1.0 eV is known from electron impact ionization[51]. But we are not aware of any report of adenine dications produced by photons, prior to our[6].

The difference-spectrum in Figure 1 shows that the dication with a mass/charge ratio of 135 u/2 e = 67.5 u/e has the fourth strongest dependence on NIR-delay, and much stronger than any other ion between 65 and 70 u/e. The existence of a 67 u ion from the XUV-photon alone however makes it difficult to judge the exact baseline level of adenine dications. An estimate after adjusting for the partly overlapping peak shapes is that the NIR-enhancement step height parameter, h, is 181±98 % of the baseline, which is two times as large as the relative enhancement for any fragment ion.

Even more interesting is that the dication enhancement starts, as seen in Figure 3, with a small but certain delay compared to the changes in most of the cationic fragment yields, when fitting the pump–probe scans data as described in the Methods section. The zeroing of the delay-axis was described in the supplement of our previous publication[6] – briefly it is given by the simultaneous increase of many cationic fragments as well as atomic krypton (the Kr^{2+} yield). The onset-time for the dication is $\tau_1 = 2.32 \pm 0.45$ fs in the previously reported experiment (one fit to the average of seven successive delay-scans)[6]. Including additional data from three other experiments performed on different days with similar conditions, we here obtain $\tau_1 = 2.42 \pm 0.80$ fs (median and sample standard deviation of fits to four experiments). τ_1 does not appear to depend on the NIR-intensity although the enhancement most likely requires the absorption of two NIR photons (based on NIR-intensity scaling and the fitted Gaussian pulse widths)[6].

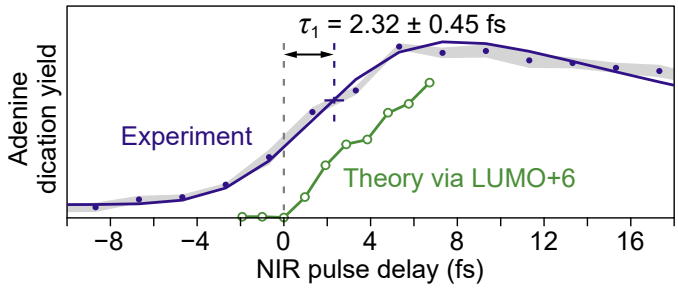

Figure 3. Delayed production of stable adenine dications. Zoom-in on the central part of a XUV-pump–NIR-probe scan[6], with experimental data points as filled circles and the fitted curve showing a significantly delayed onset (see methods section for the definition of τ_1) in the enhancement of the dication yield. The grey shaded areas show ±one standard error of the mean of 7 successive scans in alternating directions. Open circles show the main part of the theoretical result, calculated using the non-equilibrium Green's function method. The theoretical signal remains zero when the pulses fully overlap and only starts to increase at positive delays, because shake-up to the selected LUMO+6 state takes time. The result via other states does not show such a strong and late increase[6, Supplementary Fig. S18].

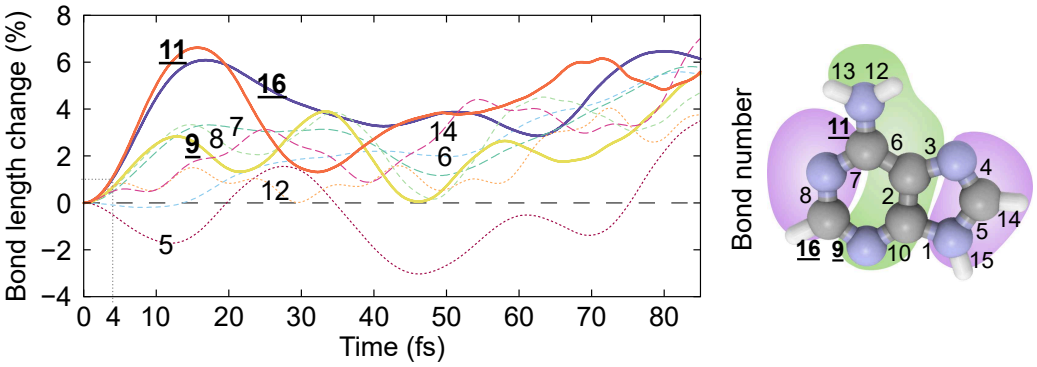

Figure 4. Bond elongation in the adenine cation. Time-dependent density functional theory Ehrenfest dynamics for the case of suddenly removing an electron from HOMO−3, illustrates the instability of the adenine cation even for near-valence excitation. In the first 4 fs, however, only 1 % elongation is reached. Bond numbers shown over each curve are defined to the right, where also the shape of HOMO−3 is shown. The curves for bonds with smaller changes are omitted for clarity.

To investigate what mechanism can be responsible for the 2.4 fs delay between XUV-photoionization and the NIR-enhanced production of dications, we explored nuclear as well as electronic dynamics in different theoretical frameworks. First of all, we verified that even if an electron is only removed from any of the four highest occupied orbitals (lowest-energy holes), the instability of the adenine cation manifests itself as a substantial bond-elongation. The result with a hole in HOMO−3, as an example, is shown in Figure 4, and several bonds oscillate and tend to elongate on a time scale of 15–85 fs (potentially proceeding towards dissociation). These calculations were made using time-dependent density functional theory (TDDFT) and Ehrenfest dynamics. We stress, however, that in the very beginning, it takes almost 4 fs before any bond has changed by 1 %, so pure nuclear dynamics is not likely to be important for the observed phenomenon.

Considering instead the electronic dynamics, we identified that a multi-electronic process can fill the initial XUV-created inner-valence hole while exciting at least one other electron to a normally unoccupied bound state. We refer to this as a *shake-up state* (although not requiring a shift in the kinetic energy of the primary photoelectron), but one can also refer to it as a frustrated Auger–Meitner-state (although no secondary electron has been emitted yet)[64, 65]. The cross-section for further photoionization by the NIR-pulse would then vary depending on the shake-up state, favouring those with one highly excited electron whose ejection is allowed in a single-active-electron picture.

We examined this proposed mechanism using two complementary theoretical frameworks, while keeping the nuclei fixed. A rate-based approach, consistent with the experimental curve model, used Fermi's golden rule and first-order perturbation theory to obtain exponential time-constants for each final-state of the highly-excited electron. More sophisticated many-body time-dependent simulations were made using a method[66, 67, 6] based on the non-equilibrium Green's function that can handle both the shake-up electron dynamics triggered by the XUV photoionization and the subsequent absorption of a delayed NIR pulse. Both these methods singled out LUMO+6 as a unique shake-up state due to rising relatively slowly but surely, while being in the energy range favoured by two-photon NIR-photoionization. The rate-equation approach gives a time-constant of about 3 fs for shake-up to LUMO+6[6, Fig. 2]. The many-body-simulated XUV+NIR signal in Figure 3 shows that the LUMO+6 contribution remains at zero when the pulses fully overlap (in contrast to an instantaneous transition which would have reached half of its peak-value) and then starts to grow nearly linearly with delay. After 4 fs it surpasses other states whose contributions stayed at a plateau reached within the first femtosecond [6, Fig. S18]. Even without discussing individual states of a particular basis set, the Green's function method allows visualization of the overall net change in electron density caused by intrinsic electronic relaxation: Figure 5(b) shows snapshots with the change in electron density as function of time, with respect to just after XUV-ionization, visualized as red (increased) or blue (decreased). The electron density more than 3 Å from the plane of the molecule is integrated and shown as a curve in Figure 5(c). It clearly grows with time. We label the vertical axis simply as "inflation" to summarize that what this observable represents is a charge migration

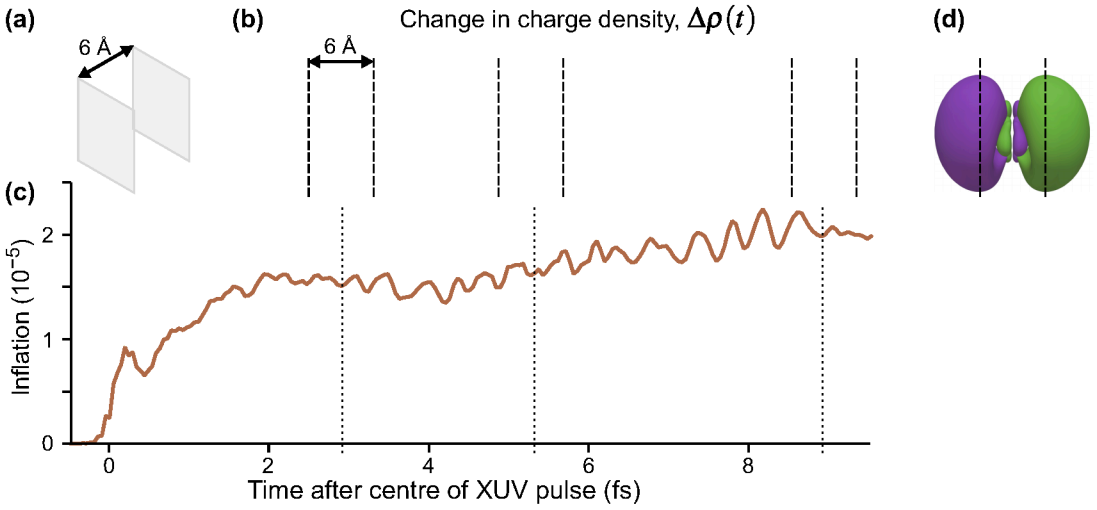

Figure 5. Charge migration in the adenine cation. (a) Illustration of the planes at 3 Å distance on either side of the molecular plane, which are used as integration boundaries for (c) and shown with dashed lines in (b) & (d). (b) Snapshots of the net change in charge density, with respect to just after the XUV-photoionization. (c) Integrated electron density more than 3 Å away from the molecular plane. The vertical axis for this dimensionless number is for brevity labelled "inflation", referring to the trend of charge migration from the central plane of the molecule to a larger volume. (d) Shape of the LUMO+6 orbital, responsible for a slowly-increasing but strong contribution to the charge migration.

from the plane of the molecule to more than 3 Å outside. Although multiple states contribute, the importance of LUMO+6 is hinted by the fact that its orbital in panel (d) has large π-like lobes on either side of the molecular plane, like the net charge migration and intuitively a large electric-dipole transition matrix element for photoionization by the NIR-pulse.

To summarize, we deduced that a specific electronic rearrangement in inner-valence-ionized adenine opens up the possibility for the NIR-pulse to create stable dications of the intact molecule. Compared with any rapidly dissociating dications[68] that might be created by the XUV-pulse directly, the route involving shake-up and NIR-photoionization must be creating dications with less excitation energy, perhaps helped by ejecting the second photoelectron. While the NIR-pulse can immediately contribute to further dissociation of adenine cations, the stabilization-enabling process takes relatively long time (τ_1 of a few femtoseconds) compared with other inner-valence electronic transitions, which makes this channel stand out in the experiment. The NIR-pulse then has to be sent before other processes, like motion of the nuclei, close the window of opportunity – the dication signal decays with $\tau_2 = 22 \pm 4$ fs. But if this sequence is completed, the resulting dication remains stable at least for the 3 µs it takes to traverse the mass spectrometer.

This combined theoretical and experimental work constitutes, to our knowledge, the first demonstration of *correlation-driven* charge migration. Conceptually it is also more of a one-way charge migration than the back-and-forth oscillation so far observed in isolated amino acids[7, 39, 40, 41] and smaller systems[8, 9]. The mere ability to resolve a transition time a few femtoseconds as non-instantaneous is testament to the usefulness of isolated attosecond pulses to investigate even molecules with as many as 15 atoms.

3.3. Time constants for dissociation channels

Figure 6 shows that the yield of several fragment ions varies in different ways as function of the XUV–NIR delay. This section will focus on the dissociation dynamics and time-constants for these photoreactions.

Starting with the τ_1-parameter that tells whether the probe's effect starts like a step function or gradually via a transition (defined on page 5), Table 1 shows a clearly nonzero τ_1 for the 70 u cation $C_2H_4N_3^+$, in addition to the previously described 2.4 fs electronic dynamics leading to the dication. The 70 u ion yield is hardly influenced by the NIR-probe at zero delay in Figure 6 but is then gradually depleted, with the time constant $\tau_1 = 9.1 \pm 5.1$ fs. The uncertainty mainly represents the possibility of a continued slope outside the scan range and an even longer τ_1 (the four experiments summarized in Table 1 gave τ_1 from 8.7 to 19.2 fs), while a shorter τ_1 would

Mass (u)	Sum formula	τ_1 (fs)	τ_2 (fs)	Step height (arb. u.)	Relative step height (%)
27	CHN^+	0.5 ± 0.2	51 ± 10	$+1.8 \pm 0.8$	$+64 \pm 16$
38	C_2N^+	0.6 ± 0.7	56 ± 32	$+1.4 \pm 0.6$	$+48 \pm 28$
43	$CH_3N_2^+$	0.9 ± 19	∞	$+0.7 \pm 0.2$	$+5 \pm 3$
53	$C_2HN_2^+$	0.7 ± 0.8	63 ± 27	$+5.2 \pm 1.5$	$+30 \pm 9$
54	$C_2H_2N_2^+$	-	-	-1.7 ± 2.4	-6 ± 9
65	$C_3HN_2^+$	0.4 ± 0.7	42 ± 27	$+0.8 \pm 0.2$	$+17 \pm 9$
66	$C_3H_2N_2^+$	28 ± 17	∞	$+0.3 \pm 0.2$	$+3 \pm 2$
70	$C_2H_4N_3^+$	9.1 ± 5.1	117 ± 326	-0.5 ± 0.4	-10 ± 6
81	$C_3H_3N_3^+$	3.0 ± 7.4	∞	-0.7 ± 0.4	-9 ± 3
92	$C_4H_2N_3^+$	5.0 ± 3.3	7.0 ± 1.5	-0.5 ± 0.2	-16 ± 8
108	$C_4H_4N_4^+$	0.4 ± 4.0	47 ± 21	-2.6 ± 1.2	-13 ± 4
135	$C_5H_5N_5^{2+}$	2.4 ± 0.8	22 ± 4	$+2.2 \pm 1.2$	$(\approx +182 \pm 99)$
135	$C_5H_5N_5^+$	-	-	-2.4 ± 3.4	-3 ± 4

Table 1. Summary of delay-dependence fitted for selected ions. The step height parameter expresses the enhancement (+) or suppression (−) before convolution with Gaussian and not limited by scan range, with respect to the baseline signal at negative NIR-delay (approximately the XUV-only signal, but for 108 u and the parent cation the baseline has a NIR-only contribution too). The table shows median values of fits to four experiments from different days with similar but not identical conditions, each containing 5, 6, 7 or 10 delay-scans. Uncertainties indicate the sample standard deviation between the four experiments and values smaller than their uncertainty are greyed out. No time constants are shown for ions without clear delay-dependence (uncertain sign of the step height). For very long decay times, ∞ is shown rather than arbitrary values ($\geq$443 fs) influenced by the chosen fitting bounds.

fail to fit the data. The 70 u fragment is one of few that require a concerted two-hydrogen migration[60], which turns the 108 u precursor ion into its lowest-energy isomer[59] and enables the dissociation path shown Figure 2(c). We can therefore speculate that the XUV-ionized molecule evolves in a way that eventually allows the NIR-absorption to suppress fragmentation into 70 u by preventing the initial hydrogen migration.

The lifetime τ_2 tells how quickly the effect of the NIR-probe decays or recovers, and values between 40 and 70 fs are found for many of the fragment ions in Table 1. Shorter lifetimes are found for the dication (22 ± 4 fs) and for the weak dip in the 92 u yield (7.0 ± 1.5 fs).

The fragment ions most strongly affected by the NIR-probe are 53 u, 108 u, 27 u and 38 u (all shown in [6]). We will here focus on 27 and 38 u which have the largest relative step heights:

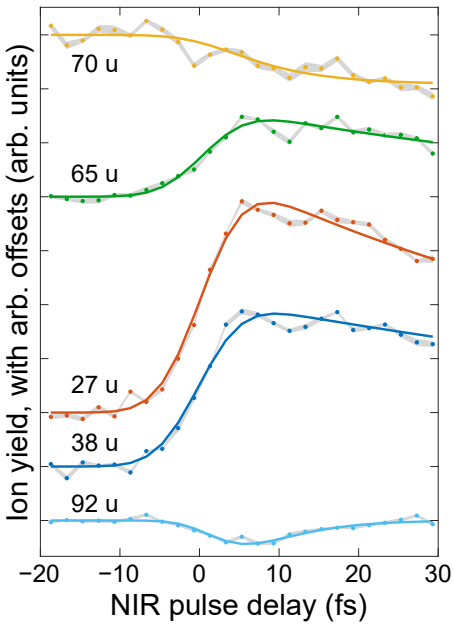

Figure 6. Delay-dependence of selected ions. The datapoints show experimental ion yields as function of XUV–NIR delay, with baselines shifted vertically for better display. The fitted model functions (see text) are shown with solid curves. The grey shaded areas show ±one standard error of the mean of 7 successive scans in alternating directions.

64 % and 48 % of their negative-delay (or XUV-only) baselines. In the following section we will also examine possible oscillations in their fragment yields.

Neutral 27 u HCN or HNC fragments appear in many dissociation paths of adenine (Figure 2). Although Figure 2(a–b) has been proposed for 27 u ions in the case of a single photon/projectile, it would be possible for a delayed NIR pulse to enhance a different reaction path which diverts charge to an otherwise neutral 27 u fragment. Since the 38 u ion has been investigated less in previous literature, we drew ellipses in Figure 2 to mark where C_2N could be produced in other ways than via the known $-NH_2$-loss sequence in Figure 2(e)[60]. We then included the suggested precursors or competing products in Table 1 to look for similarities in delay-dependence. Seeing that the 54 u yield is not influenced by the probe-pulse lets us exclude Figure 2(b & d), and that the time constants for 70 u and 43 u are very different than those for 38 u speaks against Figure 2(c). We thus conclude that 65 u is the most plausible precursor for 38 u, and it is remarkable that the complementary part of 65 u would be 27 u, i.e. 65 u could be a precursor for *both* of the fragments with the largest relative NIR-enhancement. Different isomers of 65 u appear in the (c) and (e) dissociation paths, in both cases with the breakage of a CN-bond as a final step.

3.4. Oscillating fragment yields

To examine whether there is any oscillation in the ion yields on top of the time dependence fitted in the previous section, a single-frequency oscillation was fitted to the residual datapoints, using only the part of the scan at positive NIR delay to select oscillations excited by the XUV-ionization. Such oscillations are found for the 27 u HCN^+/HNC^+ and 38 u C_2N^+ fragment yields, as shown with dashed lines in Figure 7(a). The median and standard deviations for the periods in four experiments under similar conditions are 15.0 ± 3.2 fs and 17.2 ± 3.8 fs, respectively. Oscillation periods for the other ions were not consistent between experiments, with standard deviations of 6–7 fs for two of them and exceeding 11 fs for eight of them. The 27 u and 38 u oscillations have similar periods and are initiated with approximately the same phase, having the first cosine peak at NIR-delays of 5 ± 4 and 6 ± 4 fs. This suggests that the modulating NIR-

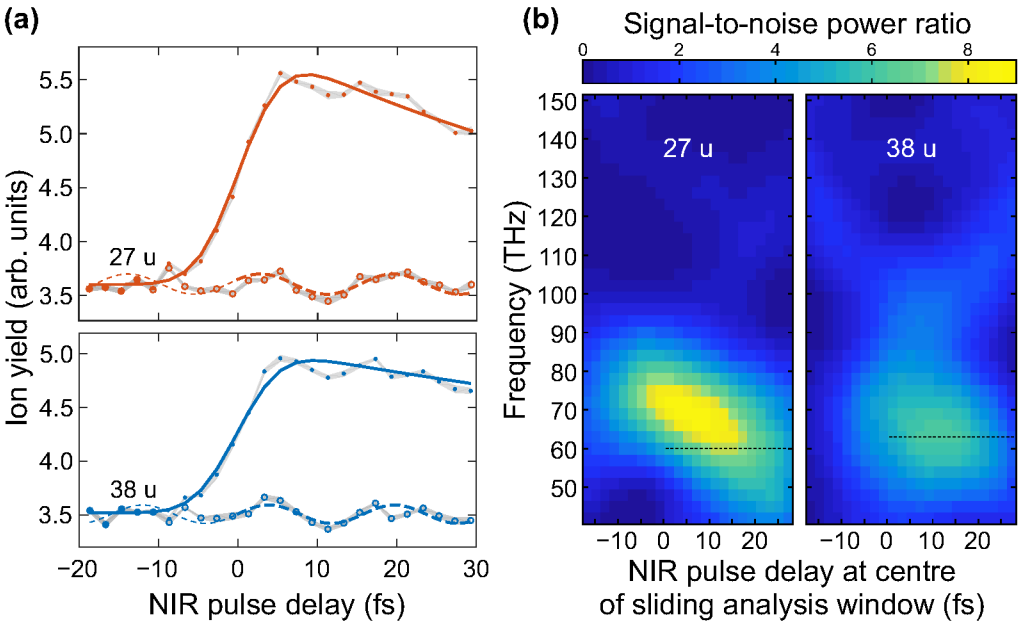

Figure 7. Oscillating ion yields. (a) Points show ion yields as function of XUV–NIR delay and solid curves show the fitted model functions of section 3.3. Circles show the residuals after subtracting the fitted curve. Thick dashed lines show cosines fitted to the residuals at positive delays (thin dashes show the extrapolation to negative delays, where no oscillation is expected). The grey shaded areas show ±one standard error of the mean of 7 successive scans in alternating directions. (b) Spectrograms using the same residual datapoints as in (a), but within a sliding 25-point Welch window (35 fs FWHM)[69]. The signal-to-noise ratio is defined as amplitude^2 of the fitted single cosine divided by the average of all datapoints' squared uncertainty. The dotted lines in (b) mark the frequencies of the oscillations in (a).

transition occurs in a common precursor rather than as a delay-dependent competition between the two fragmentation outcomes.

To investigate whether the oscillation frequency or amplitude varies during the scan, Figure 7(b) shows spectrograms computed using a sliding Welch[69] window function. Its spectral properties lie between those of the Hann and the rectangular windows[70]. We find that the oscillations are stronger when the window is centred near the end of the scan (e.g. +25 fs) than when near the start of the scan (e.g. −15 fs), which confirms that the oscillations occur in the XUV-ionized sample and are probed by the NIR-pulse (not excited by the NIR-pulse). The strongest signal/noise ratio is found at NIR-delays of 5–10 fs, near the peaks of the non-oscillating model curves in Figure 7(a).

In the frequency range of the observed oscillation, neither coherent beating between electronic states nor coherently excited vibrational wavepackets can be excluded *a priori*. The onset of nuclear motion could change the spacing between electronic states and lead to decoherence[71, 72] but the oscillation amplitude remains roughly constant for at least as long as the τ_2 lifetime of the non-oscillating step. While a time-dependent localization of charge on the 27 u-side in the dissociation Figure 2(a) could probably modulate the 27 u ion yield, there does not appear to be any such immediate path towards charged 38 u fragments. Considering these arguments and the difficulty of simulating coherent electronic dynamics while letting the nuclei move, we will in the following focus on a vibrational assignment.

The observed oscillation frequency is consistent with the general band for CN-stretching vibrations, possibly in the 65 u precursor and certainly in the neutral 27 u and 38 u fragments (16 fs for HN–C [73] and HC–N [74], 17 fs for C–C–N asymmetric stretch[75, 76]). Although NIR-photoionization of electronically excited fragments could have a cross section dependent on their bond lengths, such an assignment is difficult to reconcile with the immediate onset of the oscillations. In particular, the 38 u fragment shown in Figure 2 can not be formed without substantial nuclear motion[60, 58], which must be expected to take time.

To get an idea of which bonds start to elongate *quickly*, and better support a vibrational explanation, we revisit Figure 4 and our TDDFT Ehrenfest dynamics calculations for the adenine cation[6, Supplementary Figure S10]. Two CN-bonds in the backbone show rapid elongation: bond #9 relating to Figure 2(a) and bond #11 which concerns the –NH_2-group which has already been highlighted in the dissociation path in Figure 2(e). Figure 4 shows that the C–NH_2 bond #11 elongates dramatically by 6.5 % in 15 fs after sudden removal of an electron from HOMO−3. The simulation as well as vibronic spectroscopy on adenine[77, 78] give period times of 30–33 fs for this bond, so its second overtone would match the ion yield oscillations perfectly. A coherent comb beating at twice the fundamental frequency could possibly be excited if only the even-numbered vibrational levels have nonzero Franck–Condon factors[79] (or classically by a transition occurring only at the equilibrium geometry twice per oscillation period). Within the experimental uncertainty, a directly matching fundamental 20 fs oscillation period has also been reported for a mode that involves both the C–NH_2 stretch and NH_2 scissoring[80, 81, 82]. (An even better matching peak at 17 fs, 1909 cm^{-1}, in calculations of Nowak *et al.*[82] was weak and not assigned.)

4. Conclusions

To control photochemical reactions requires a thorough understanding of both electronic and vibrational dynamics. The greatest challenges for theoretical work can be found at ultrafast time scales, in energy-ranges where electronic correlation is important (inner-valence holes) and with large molecules. In this work we time-resolved different types of relaxation processes in the nucleobase adenine ($C_5H_5N_5$) after photoionization in the previously unexplored extreme ultraviolet energy range, also relevant for DNA-damage by secondary electrons in tissue.

Our XUV-pump – NIR-probe experiment provides onset- and decay-times of molecular processes which are revealed by how the yields of the intact adenine dication and several fragment ions are influenced by the NIR pulse at different time delays. Although the precise non-adiabatic mechanisms responsible for their decays were not elucidated, assignments were given for the few-femtosecond delayed onsets discovered for the 70 u $C_2H_4N_3^+$ fragment ion and the dication ($C_5H_5N_5^{2+}$). The former may be related to double hydrogen-migration that is required to form $C_2H_4N_3^+$. The latter was assigned as a kind of charge migration with the help of first-principles theory and represents the first time that a multi-electronic process in a polyatomic molecule

has been tracked in real time[6]. The time required for the charge migration let us achieve a degree of control of the yield of intact dications via the XUV–NIR delay parameter and the ability to resolve the phenomenon as non-instantaneous demonstrates the potential of attosecond technology even for molecules with as many as 15 atoms.

Furthermore, we propose that delay-dependent oscillations in the yields of the 27 u CHN^+ and 38 u C_2N^+ fragment ions may be a consequence of C–NH_2-stretching vibrations in the adenine cation. The XUV attosecond pulse excites a broadband coherent vibrational wavepacket whose beating, as function of delay before the NIR-probe is absorbed, may modulate the probability of entering the dissociation path in Figure 2(e) where loss of NH_2 is necessary. The similar oscillation amplitudes for HCN^+ and C_2N^+ suggest that a similar number of steps are required, i.e. that the oscillating HCN^+ is formed after hydrogen migration together with a neutral 65 or 38 u, rather than directly with 92 u.

In summary, by controlling when the NIR-pulse is sent with extreme time resolution we have been able to suppress and enhance different molecular dissociation channels, both in a conventional way by exploiting vibronic dynamics and in a novel way based on pure electronic dynamics. This is promising for the outlook of controlling photochemistry at its natural time scale[10, 12].

5. Acknowledgments

F.Ca. acknowledges support from the European Research Council under the ERC-2014-StG STARLIGHT (Grant Agreement No. 637756). F. Ca and A. R. acknowledge support from the Deutsche Forschungsgemeinschaft (DFG, German Research Foundation) – SFB-925 – project 170620586 and the Cluster of Excellence Advanced Imaging of Matter (AIM). F.L. and V.W. acknowledge the Fonds de recherche du Québec – Nature et technologies (FRQNT) and the National Science and Engineering Research Council (NSERC). V.W. acknowledges support from the Vanier Canada Graduate Scholarship (Vanier CGS) program. A.T. acknowledges support from the Helmholtz association under the Helmholtz Young Investigator Group VH-NG-1613. S. L. acknowledges support from the Alexander von Humboldt foundation. A. R. acknowledge financial support from the European Research Council(ERC-2015-AdG-694097). The Flatiron Institute is a division of the Simons Foundation. G.S. and E.P. acknowledge EC funding through the RISE Co-ExAN (Grant No. GA644076), the European Union project MaX Materials design at the eXascale H2020- EINFRA-2015-1, Grant Agreement No. 676598, Nanoscience Foundries and Fine Analysis-Europe H2020-INFRAIA-2014-2015, Grant Agreement No. 654360 and Tor Vergata University for financial support through the Mission Sustainability Project 2DUTOPI. E.P., G.S. and M.N. acknowledge funding from MIUR PRIN, Grant No. 20173B72NB. J. B. G. acknowledge support from the EPSRC (UK) grant number EP/M001644/1.

6. Data availability statement

The data that support the findings of this study are available from the corresponding author upon reasonable request.

Appendix A. Fitting and statistics

For each experiment, ion yields from multiple delay-scans are averaged and errorbars defined by the standard error of the mean. The curve model introduced on page 5 is expanded for a global fit of the delay-dependent signals for all the analysed ions, where the pulse duration is a shared parameter and each ion has individual parameters for baseline, step height, exponential onset-time τ_1 and exponential decay-time τ_2.

The Gaussian for each signal has a full-width at half-max $W/\sqrt{n_i}$ where W represents NIR pulse duration and n_i is the number of NIR-photons absorbed for the signal of ion i (usually 1 but chosen as 2 for 92 u, 108 u and the adenine dication). The zeroing of the delay-axis can be fitted as an additional common parameter but for the main experiment it is held fixed to agree exactly with our previous publication[6] (would otherwise vary on the 0.1-fs level depending on which ions are included in the global fit). Additionally, we have here considered three similar experiments to check the robustness and provide median-values and sample standard deviations of fitted parameters.

For oscillations fitted to residuals beyond the above curve model, significance can be judged via the signal-to-noise power ratio (computed as the fitted cosine's squared amplitude divided by the average of all datapoints' squared signal-errorbars). Its statistical distribution is known for the null hypothesis of no real signal, so for a p-value of 5 % a signal-to-noise ratio of 6.6 is considered significant, including the correction[83] for examining multiple frequencies (37 here, in steps of 3 THz from 42 to 150 THz). Additionally, we compute the difference in corrected Akaike Information Criterion (dAICc)[84] with the sign chosen to be positive if the cosine model function is preferred over a single-parameter constant model. The residual oscillations in Figure 7(a) for 27 u and 38 u have the respective signal-to-noise ratios 7.7 and 7.5 (corresponding to p-values of 0.017 and 0.020) and dAICc-values of 4.7 and 8.4.

References

[1] Ahmed H. Zewail. Femtochemistry: Atomic-scale dynamics of the chemical bond using ultrafast lasers (Nobel lecture). *Angewandte Chemie International Edition*, 39(15):2586–2631, 2000.

[2] M. Gruebele and A. H. Zewail. Femtosecond wave packet spectroscopy: Coherences, the potential, and structural determination. *The Journal of Chemical Physics*, 98(2):883–902, 1993.

[3] M. Drescher, M. Hentschel, R. Kienberger, M. Uiberacker, V. Yakovlev, A. Scrinzi, Th. Westerwalbesloh, U. Kleineberg, U. Heinzmann, and F. Krausz. Time-resolved atomic inner-shell spectroscopy. *Nature*, 419(6909):803–807, 2002.

[4] Athiya Mahmud Hanna, Oriol Vendrell, Abbas Ourmazd, and Robin Santra. Laser control over the ultrafast Coulomb explosion of $N_2{}^{2+}$ after Auger decay: A quantum-dynamics investigation. *Physical Review A*, 95(4):043419, 2017.

[5] M. Uiberacker, Th. Uphues, M. Schultze, A. J. Verhoef, V. Yakovlev, M. F. Kling, J. Rauschenberger, N. M. Kabachnik, H. Schröder, M. Lezius, K. L. Kompa, H.-G. Muller, M. J. J. Vrakking, S. Hendel, U. Kleineberg, U. Heinzmann, M. Drescher, and F. Krausz. Attosecond real-time observation of electron tunnelling in atoms. *Nature*, 446(7136):627–632, 2007.

[6] Erik P. Månsson, Simone Latini, Fabio Covito, Vincent Wanie, Mara Galli, Enrico Perfetto, Gianluca Stefanucci, Hannes Hübener, Umberto De Giovannini, Mattea C. Castrovilli, Andrea Trabattoni, Fabio Frassetto, Luca Poletto, Jason B. Greenwood, François Légaré, Mauro Nisoli, Angel Rubio, and Francesca Calegari. Real-time observation of a correlation-driven sub 3 fs charge migration in ionised adenine. *Communications Chemistry*, 4(1), 2021.

[7] F. Calegari, D. Ayuso, A. Trabattoni, L. Belshaw, S. De Camillis, S. Anumula, F. Frassetto, L. Poletto, A. Palacios, P. Decleva, J. B. Greenwood, F. Martín, and M. Nisoli. Ultrafast electron dynamics in phenylalanine initiated by attosecond pulses. *Science*, 346(6207):336–339, 2014.

[8] P. Ranitovic, C. W. Hogle, P. Riviere, A. Palacios, X.-M. Tong, N. Toshima, A. Gonzalez-Castrillo, L. Martin, F. Martin, M. M. Murnane, and H. Kapteyn. Attosecond vacuum UV coherent control of molecular dynamics. *PNAS*, 111(3):912–917, 2014.

[9] P. M. Kraus, B. Mignolet, D. Baykusheva, A. Rupenyan, L. Horný, E. F. Penka, G. Grassi, O. I. Tolstikhin, J. Schneider, F. Jensen, L. B. Madsen, A. D. Bandrauk, F. Remacle, and H. J. Wörner. Measurement and laser control of attosecond charge migration in ionized iodoacetylene. *Science*, 350(6262):790–795, 2015.

[10] Alicia Palacios and Fernando Martín. The quantum chemistry of attosecond molecular science. *WIREs Computational Molecular Science*, 10(1), 2019.

[11] Peter M. Kraus and Hans Jakob Wörner. Perspectives of attosecond spectroscopy for the understanding of fundamental electron correlations. *Angewandte Chemie International Edition*, 57(19):5228–5247, 2018.

[12] Franck Lépine, Misha Y. Ivanov, and Marc J. J. Vrakking. Attosecond molecular dynamics: fact or fiction? *Nature Photonics*, 8(3):195–204, 2014.

[13] Linda Young, Kiyoshi Ueda, Markus Gühr, Philip H Bucksbaum, Marc Simon, Shaul Mukamel, Nina Rohringer, Kevin C. Prince, Claudio Masciovecchio, Michael Meyer, Artem Rudenko, Daniel Rolles, Christoph Bostedt, Matthias Fuchs, David A. Reis, Robin Santra, Henry Kapteyn, Margaret Murnane, Heide Ibrahim, François Légaré, Marc Vrakking, Marcus Isinger, David Kroon, Mathieu Gisselbrecht, Anne L'Huillier, Hans Jakob Wörner, and Stephen R. Leone. Roadmap of ultrafast x-ray atomic and molecular physics. *J. Phys. B: At., Mol. Opt. Phys.*, 51(3):032003, 2018.

[14] M. Lewenstein, Ph. Balcou, M. Yu. Ivanov, Anne L'Huillier, and P. B. Corkum. Theory of high-harmonic generation by low-frequency laser fields. *Phys. Rev. A*, 49:2117–2132, Mar 1994.

[15] Mauro Nisoli, Piero Decleva, Francesca Calegari, Alicia Palacios, and Fernando Martín. Attosecond electron dynamics in molecules. *Chemical Reviews*, 117(16):10760–10825, 2017.

[16] M. Hentschel, R. Kienberger, Ch. Spielmann, G. A. Reider, N. Milosevic, T. Brabec, P. Corkum, U. Heinzmann, M. Drescher, and F. Krausz. Attosecond metrology. *Nature*, 414:509–513, 2001.

[17] J. Itatani, F. Quéré, G. L. Yudin, M. Yu. Ivanov, F. Krausz, and P. B. Corkum. Attosecond streak camera. *Physical Review Letters*, 88(17), 2002.

[18] H.G. Muller. Reconstruction of attosecond harmonic beating by interference of two-photon transitions. *Applied Physics B*, 74(S1):s17–s21, 2002.

[19] J M Dahlström, A L'Huillier, and A Maquet. Introduction to attosecond delays in photoionization. *J. Phys. B: At., Mol. Opt. Phys.*, 45(18):183001, August 2012.

[20] M. Ossiander, F. Siegrist, V. Shirvanyan, R. Pazourek, A. Sommer, T. Latka, A. Guggenmos, S. Nagele, J. Feist, J. Burgdörfer, R. Kienberger, and M. Schultze. Attosecond correlation dynamics. *Nature Physics*, 13(3):280–285, 2016.

[21] Claudio Cirelli, Carlos Marante, Sebastian Heuser, C. L. M. Petersson, Álvaro Jiménez Galán, Luca Argenti,

Shiyang Zhong, David Busto, Marcus Isinger, Saikat Nandi, Sylvain Maclot, Linnea Rading, Per Johnsson, Mathieu Gisselbrecht, Matteo Lucchini, Lukas Gallmann, J. Marcus Dahlström, Eva Lindroth, Anne L'Huillier, Fernando Martín, and Ursula Keller. Anisotropic photoemission time delays close to a Fano resonance. *Nature Communications*, 9(1), mar 2018.

[22] Erik P. Månsson, Diego Guénot, Cord L. Arnold, David Kroon, Susan Kasper, J. Marcus Dahlström, Eva Lindroth, Anatoli S. Kheifets, Anne L'Huillier, Stacey L. Sorensen, and Mathieu Gisselbrecht. Double ionization probed on the attosecond timescale. *Nature Physics*, 10(3):207–211, jan 2014.

[23] L. Cattaneo, J. Vos, R. Y. Bello, A. Palacios, S. Heuser, L. Pedrelli, M. Lucchini, C. Cirelli, F. Martín, and U. Keller. Attosecond coupled electron and nuclear dynamics in dissociative ionization of H2. *Nature Physics*, 14(7):733–738, 2018.

[24] S. Nandi, E. Plésiat, S. Zhong, A. Palacios, D. Busto, M. Isinger, L. Neoričić, C. L. Arnold, R. J. Squibb, R. Feifel, P. Decleva, A. L'Huillier, F. Martín, and M. Gisselbrecht. Attosecond timing of electron emission from a molecular shape resonance. *Science Advances*, 6(31):eaba7762, jul 2020.

[25] Inga Jordan, Martin Huppert, Dominik Rattenbacher, Michael Peper, Denis Jelovina, Conaill Perry, Aaron von Conta, Axel Schild, and Hans Jakob Wörner. Attosecond spectroscopy of liquid water. *Science*, 369(6506):974–979, 2020.

[26] Wei Quan, Vladislav V. Serov, MingZheng Wei, Meng Zhao, Yu Zhou, YanLan Wang, XuanYang Lai, Anatoli S. Kheifets, and XiaoJun Liu. Attosecond molecular angular streaking with all-ionic fragments detection. *Physical Review Letters*, 123(22), nov 2019.

[27] Jaco Fuchs, Nicolas Douguet, Stefan Donsa, Fernando Martin, Joachim Burgdörfer, Luca Argenti, Laura Cattaneo, and Ursula Keller. Time delays from one-photon transitions in the continuum. *Optica*, 7(2):154, 2020.

[28] Romain Geneaux, Hugo J. B. Marroux, Alexander Guggenmos, Daniel M. Neumark, and Stephen R. Leone. Transient absorption spectroscopy using high harmonic generation: a review of ultrafast x-ray dynamics in molecules and solids. *Phil. Trans. R. Soc. A*, 377:20170463, 2019.

[29] R. Berera, van R. Grondelle, and J.T.M. Kennis. Ultrafast transient absorption spectroscopy: principles and application to photosynthetic systems. *Photosynthesis Research*, 101:105–118, 2009.

[30] G. Grégoire, H. Kang, C. Dedonder-Lardeux, C. Jouvet, C. Desfrançois, D. Onidas, V. Lepere, and J. A. Fayeton. Statistical vs. non-statistical deactivation pathways in the UV photo-fragmentation of protonated tryptophan–leucinedipeptide. *Phys. Chem. Chem. Phys.*, 8(1):122–128, 2006.

[31] Benjamin Erk, Rebecca Boll, Sebastian Trippel, Denis Anielski, Lutz Foucar, Benedikt Rudek, Sascha W. Epp, Ryan Coffee, Sebastian Carron, Sebastian Schorb, Ken R. Ferguson, Michele Swiggers, John D. Bozek, Marc Simon, Tatiana Marchenko, Jochen Küpper, Ilme Schlichting, Joachim Ullrich, Christoph Bostedt, Daniel Rolles, and Artem Rudenko. Imaging charge transfer in iodomethane upon x-ray photoabsorption. *Science*, 345(6194):288–291, jul 2014.

[32] Marius Hervé, Alexie Boyer, Richard Brédy, Isabelle Compagnon, Abdul-Rahman Allouche, and Franck Lépine. Controlled ultrafast $\pi\pi^*$–$\pi\sigma^*$ dynamics in tryptophan-based peptides with tailored micro-environment. *Communications Chemistry*, 4(1), 2021.

[33] Henning Zettergren, Alicja Domaracka, Thomas Schlathölter, Paola Bolognesi, Sergio Díaz-Tendero, Marta Łabuda, Sanja Tosic, Sylvain Maclot, Per Johnsson, Amanda Steber, Denis Tikhonov, Mattea Carmen Castrovilli, Lorenzo Avaldi, Sadia Bari, Aleksandar R. Milosavljević, Alicia Palacios, Shirin Faraji, Dariusz G. Piekarski, Patrick Rousseau, Daniela Ascenzi, Claire Romanzin, Ewa Erdmann, Manuel Alcamí, Janina Kopyra, Paulo Limão-Vieira, Jaroslav Kočišek, Juraj Fedor, Simon Albertini, Michael Gatchell, Henrik Cederquist, Henning T. Schmidt, Elisabeth Gruber, Lars H. Andersen, Oded Heber, Yoni Toker, Klavs Hansen, Jennifer A. Noble, Christophe Jouvet, Christina Kjær, Steen Brøndsted Nielsen, Eduardo Carrascosa, James Bull, Alessandra Candian, and Annemieke Petrignani. Roadmap on dynamics of molecules and clusters in the gas phase. *The European Physical Journal D*, 75(5), may 2021.

[34] Lorenz S Cederbaum and J. Zobeley. Ultrafast charge migration by electron correlation. *Chemical Physics Letters*, 307(3-4):205–210, 1999.

[35] Hans Jakob Wörner, Christopher A. Arrell, Natalie Banerji, Andrea Cannizzo, Majed Chergui, Akshaya K. Das, Peter Hamm, Ursula Keller, Peter M. Kraus, Elisa Liberatore, Pablo Lopez-Tarifa, Matteo Lucchini, Markus Meuwly, Chris Milne, Jacques-E. Moser, Ursula Rothlisberger, Grigory Smolentsev, Joël Teuscher, Jeroen A. van Bokhoven, and Oliver Wenger. Charge migration and charge transfer in molecular systems. *Structural Dynamics*, 4(6):061508, 2017.

[36] R. Weinkauf, P. Schanen, A. Metsala, E. W. Schlag, M. Bürgle, and H. Kessler. Highly efficient charge transfer in peptide cations in the gas phase: threshold effects and mechanism. *The Journal of Physical Chemistry*, 100(47):18567–18585, 1996.

[37] Alexander I. Kuleff and Lorenz S. Cederbaum. Ultrafast correlation-driven electron dynamics. *J. Phys. B: At., Mol. Opt. Phys.*, 47(12):124002, 2014.

[38] F. Remacle and R. D. Levine. An electronic time scale in chemistry. *PNAS*, 103(18):6793–6798, 2006.

[39] A. Trabattoni, M. Galli, M. Lara-Astiaso, A. Palacios, J. Greenwood, I. Tavernelli, P. Decleva, M. Nisoli, F. Martín, and F. Calegari. Charge migration in photo-ionized aromatic amino acids. *Philosophical Transactions of the Royal Society A: Mathematical, Physical and Engineering Sciences*, 377(2145):20170472, 2019.

[40] Manuel Lara-Astiaso, Mara Galli, Andrea Trabattoni, Alicia Palacios, David Ayuso, Fabio Frassetto, Luca Poletto, Simone De Camillis, Jason Greenwood, Piero Decleva, Ivano Tavernelli, Francesca Calegari, Mauro Nisoli, and Fernando Martín. Attosecond pump–probe spectroscopy of charge dynamics in tryptophan. *The Journal of Physical Chemistry Letters*, 9(16):4570–4577, 2018.

[41] Manuel Lara-Astiaso, Alicia Palacios, Piero Decleva, Ivano Tavernelli, and Fernando Martín. Role of electron-nuclear coupled dynamics on charge migration induced by attosecond pulses in glycine. *Chemical Physics Letters*, 683:357–364, 2017. Ahmed Zewail (1946-2016) Commemoration Issue of Chemical Physics Letters.

[42] Fatemeh Khalili, Mohsen Vafaee, and Babak Shokri. Attosecond charge migration following oxygen K-shell ionization in DNA bases and base pairs. *Phys. Chem. Chem. Phys.*, 2021.

[43] Michael A. Huels, Badia Boudaïffa, Pierre Cloutier, Darel Hunting, and Leon Sanche. Single, double, and multiple double strand breaks induced in DNA by 3–100 eV electrons. *Journal of the American Chemical Society*, 125(15):4467–4477, 2003.

[44] T. Jahnke, H. Sann, T. Havermeier, K. Kreidi, C. Stuck, M. Meckel, M. Schöffler, N. Neumann, R. Wallauer, S. Voss, A. Czasch, O. Jagutzki, A. Malakzadeh, F. Afaneh, Th. Weber, H. Schmidt-Böcking, and R. Dörner. Ultrafast energy transfer between water molecules. *Nature Physics*, 6(2):139–142, 2010.

[45] Melanie Mucke, Markus Braune, Silko Barth, Marko Förstel, Toralf Lischke, Volker Ulrich, Tiberiu Arion, Uwe Becker, Alex Bradshaw, and Uwe Hergenhahn. A hitherto unrecognized source of low-energy electrons in water. *Nature Physics*, 6(2):143–146, 2010.

[46] Thomas Gustavsson, Roberto Improta, and Dimitra Markovitsi. DNA/RNA: Building blocks of life under UV irradiation. *The Journal of Physical Chemistry Letters*, 1(13):2025–2030, 2010.

[47] Hui Yu, Jose A. Sanchez-Rodriguez, Marvin Pollum, Carlos E. Crespo-Hernández, Sebastian Mai, Philipp Marquetand, Leticia González, and Susanne Ullrich. Internal conversion and intersystem crossing pathways in uv excited, isolated uracils and their implications in prebiotic chemistry. *Phys. Chem. Chem. Phys.*, 18:20168–20176, 2016.

[48] Arthur Kuhlmann, Larissa Bihr, and Hans-Achim Wagenknecht. How far does energy migrate in DNA and cause damage? evidence for long-range photodamage to DNA. *Angewandte Chemie International Edition*, 59(40):17378–17382, 2020.

[49] A. Muñoz, J. C. Oller, F. Blanco, J. D. Gorfinkiel, P. Limão-Vieira, and G. García. Electron-scattering cross sections and stopping powers in H_2O. *Physical Review A*, 76(5):052707, 2007.

[50] E. P. Månsson, S. De Camillis, M. C. Castrovilli, M. Galli, M. Nisoli, F. Calegari, and J. B. Greenwood. Ultrafast dynamics in the DNA building blocks thymidine and thymine initiated by ionizing radiation. *Phys. Chem. Chem. Phys.*, 19:19815–19821, 2017.

[51] Peter J. M. van der Burgt, Sinead Finnegan, and Samuel Eden. Electron impact fragmentation of adenine: partial ionization cross sections for positive fragments. *The European Physical Journal D*, 69(7):173, 2015.

[52] M. Nisoli, S. De Silvestri, and O. Svelto. Generation of high energy 10 fs pulses by a new pulse compression technique. *Applied Physics Letters*, 68(20):2793–2795, 1996.

[53] M. Nisoli, S. De Silvestri, O. Svelto, R. Szipöcs, K. Ferencz, Ch. Spielmann, S. Sartania, and F. Krausz. Compression of high-energy laser pulses below 5 fs. *Optics Letters*, 22(8):522, 1997.

[54] I. J. Sola, E. Mével, L. Elouga, E. Constant, V. Strelkov, L. Poletto, P. Villoresi, E. Benedetti, J.-P. Caumes, S. Stagira, C. Vozzi, G. Sansone, and M. Nisoli. Controlling attosecond electron dynamics by phase-stabilized polarization gating. *Nature Physics*, 2(5):319–322, 2006.

[55] G. Sansone, E. Benedetti, F. Calegari, C. Vozzi, L. Avaldi, R. Flammini, L. Poletto, P. Villoresi, C. Altucci, R. Velotta, S. Stagira, S. De Silvestri, and M. Nisoli. Isolated single-cycle attosecond pulses. *Science*, 314(5798):443–446, oct 2006.

[56] Francesca Calegari, Giuseppe Sansone, Salvatore Stagira, Caterina Vozzi, and Mauro Nisoli. Advances in attosecond science. *J. Phys. B: At., Mol. Opt. Phys.*, 49(6):062001, 2016.

[57] Rodrigo López-Martens, Katalin Varjú, Per Johnsson, Johan Mauritsson, Yann Mairesse, Pascal Salières, Mette B. Gaarde, Kenneth J. Schafer, Anders Persson, Sune Svanberg, Claes-Göran Wahlström, and Anne L'Huillier. Amplitude and phase control of attosecond light pulses. *Physical Review Letters*, 94(3), 2005.

[58] Christoph Alexander Bauer and Stefan Grimme. Elucidation of electron ionization induced fragmentations of adenine by semiempirical and density functional molecular dynamics. *The Journal of Physical Chemistry A*, 118(49):11479–11484, 2014.

[59] B. F. Minaev, M. I. Shafranyosh, Yu. Yu Svida, M. I. Sukhoviya, I. I. Shafranyosh, G. V. Baryshnikov, and V. A. Minaeva. Fragmentation of the adenine and guanine molecules induced by electron collisions. *The Journal of Chemical Physics*, 140(17):175101, 2014.

[60] Hans-Werner Jochims, Martin Schwell, Helmut Baumgärtel, and Sydney Leach. Photoion mass spectrometry of adenine, thymine and uracil in the 6–22eV photon energy range. *Chemical Physics*, 314(1-3):263–282, 2005.

[61] S. Pilling, A. F. Lago, L. H. Coutinho, R. B. de Castilho, G. G. B. de Souza, and A. Naves de Brito. Dissociative photoionization of adenine following valence excitation. *Rapid Communications in Mass Spectrometry*, 21(22):3646–3652, 2007.

[62] Jerry M. Rice and Gerald O. Dudek. Mass spectra of nucleic acid derivatives. II. Guanine, adenine, and related compounds. *Journal of the American Chemical Society*, 89(11):2719–2725, 1967.

[63] Fresia Alvarado, Sadia Bari, Ronnie Hoekstra, and Thomas Schlathölter. Interactions of neutral and singly charged keV atomic particles with gas-phase adenine molecules. *The Journal of Chemical Physics*, 127(3):034301, 2007.

[64] Paul S. Bagus, R. Broer, and Eugene S. Ilton. A new near degeneracy effect for photoemission in transition metals. *Chemical Physics Letters*, 394(1):150–154, 2004.

[65] Victor Despré and Alexander I. Kuleff. Correlation-driven charge migration as initial step in the dynamics in correlation bands, 2021.

[66] E. Perfetto and G. Stefanucci. CHEERS: a tool for correlated hole-electron evolution from real-time simulations. *Journal of Physics: Condensed Matter*, 30(46):465901, 2018.

[67] F Covito, E Perfetto, A Rubio, and G Stefanucci. Real-time dynamics of Auger wave packets and decays in ultrafast charge migration processes. *Physical Review A*, 97(6):061401, 2018.

[68] Patrick Moretto-Capelle, Arnaud Le Padellec, Guillaume Brière, Sophie Massou, and Frédéric Franceries. Energetics and metastability of the adenine dication observed in proton-adenine collisions. *The Journal of Chemical Physics*, 127(23):234311, 2007.

[69] P. Welch. The use of fast Fourier transform for the estimation of power spectra: A method based on time averaging over short, modified periodograms. *IEEE Transactions on Audio and Electroacoustics*, 15(2):70–73, 1967.

[70] Gerhard Heinzel, Albrecht Rüdiger, and Roland Schilling. Spectrum and spectral density estimation by

the discrete fourier transform (DFT), including a comprehensive list of window functions and some new at-top windows. techreport, Laser Interferometry & Gravitational Wave Astronomy, AEI-Hannover, MPI for Gravitational Physics, 2002.

[71] Morgane Vacher, Lee Steinberg, Andrew J. Jenkins, Michael J. Bearpark, and Michael A. Robb. Electron dynamics following photoionization: Decoherence due to the nuclear-wave-packet width. *Physical Review A*, 92(4), oct 2015.

[72] Maximilian Hollstein, Robin Santra, and Daniela Pfannkuche. Correlation-driven charge migration following double ionization and attosecond transient absorption spectroscopy. *Physical Review A*, 95:053411, 2017.

[73] Daniel Forney, Warren E. Thompson, and Marilyn E. Jacox. The vibrational spectra of molecular ions isolated in solid neon. IX. HCN^+, HNC^+, and CN^-. *The Journal of Chemical Physics*, 97(3):1664–1674, 1992.

[74] Peter Linstrom and W. G. Mallard. Nist chemistry webbook, nist standard reference database 69. (Eds.), 1997.

[75] M. Fehér, C. Salud, and J.P. Maier. The infrared laser spectrum of the ν_1 band of CCN. *Journal of Molecular Spectroscopy*, 145(2):246–250, 1991.

[76] A. M. Mebel and R. I. Kaiser. The formation of interstellar C_2N isomers in circumstellar envelopes of carbon stars: An ab initio study. *The Astrophysical Journal*, 564(2):787–791, 2002.

[77] Z. Dhaouadi, M. Ghomi, J. C. Austin, R. B. Girling, R. E. Hester, P. Mojzes, L. Chinsky, P. Y. Turpin, C. Coulombeau, H. Jobic, and J. Tomkinson. Vibrational motions of bases of nucleic acids as revealed by neutron inelastic scattering and resonance Raman spectroscopy. 1. Adenine and its deuterated species. *The Journal of Physical Chemistry*, 97(5):1074–1084, 1993.

[78] K. Laamiri, G. A. Garcia, L. Nahon, A. Ben Houria, R. Feifel, and M. Hochlaf. Threshold photoelectron spectroscopy of 9-methyladenine: theory and experiment. *Phys. Chem. Chem. Phys.*, 2021.

[79] Chih-Kai Lin, Ming-Chung Li, Masahiro Yamaki, Michitoshi Hayashi, and Sheng Hsien Lin. A theoretical study on the spectroscopy and the radiative and non-radiative relaxation rate constants of the $s_0^1a_1$–$s_1^1a_2$ vibronic transitions of formaldehyde. *Phys. Chem. Chem. Phys.*, 12(37):11432, 2010.

[80] Antonio Rodes, Manuela Rueda, Francisco Prieto, César Prado, Juan Miguel Feliu, and Antonio Aldaz. Adenine adsorption at single crystal and thin-film gold electrodes: An in situ infrared spectroscopy study. *Journal of Physical Chemistry C*, 113(43):18784–18794, 2009.

[81] Rui P. Lopes, Rosendo Valero, John Tomkinson, M. Paula M. Marques, and Luís A. E. Batista de Carvalho. Applying vibrational spectroscopy to the study of nucleobases – adenine as a case-study. *New Journal of Chemistry*, 37(9):2691, 2013.

[82] Maciej J. Nowak, Leszek Lapinski, Józef S. Kwiatkowski, and Jerzy Leszczyński. Molecular structure and infrared spectra of adenine. Experimental matrix isolation and density functional theory study of adenine ^{15}N isotopomers. *Journal of Physical Chemistry*, 100(9):3527–3534, 1996.

[83] J. D. Scargle. Studies in astronomical time series analysis. II - statistical aspects of spectral analysis of unevenly spaced data. *Astrophysical Journal*, 263:835–853, 1982.

[84] Kenneth P. Burnham and David R. Anderson. Multimodel inference. *Sociological Methods & Research*, 33(2):261–304, 2004.